ANL/ED/CP-100464

MORPHOLOGIES OF URANIUM DEPOSITS PRODUCED DURING ELECTROREFINING OF EBR-II SPENT NUCLEAR FUEL

by

Terry C. Totemeier

Engineering Division
Argonne National Laboratory-West
P. O. Box 2528
Idaho Falls, ID 8343-2528

Embedded Topical Meeting on DOE Spent Fuel and Fissile Material Management
San Diego, CA

June 4-8, 2000

*Work supported by the U.S. Department of Energy, Materials/Chemistry, Materials Characterization, under Contract W-31-109-ENG-38.

DISCLAIMER

MORPHOLOGIES OF URANIUM DEPOSITS PRODUCED DURING ELECTROREFINING OF EBR-II SPENT NUCLEAR FUEL

Terry C. Totemeier
Argonne National Laboratory
Idaho Falls, ID 83403-2528
(208) 533-7458

Nancy L. Dietz
Argonne National Laboratory
Idaho Falls, ID 83403-2528
(208) 533-7469

ABSTRACT

The morphologies of U metal samples from deposits produced by electrorefining of Experimental Breeder Reactor-II (EBR-II) spent fuel were examined using scanning electron microscopy, energy- and wavelength-dispersive X-ray spectroscopy, and metallography. The morphologies were analyzed to find correlations with the chemistry of the samples, the ER run conditions, and the deposit performance. A rough correlation was observed between morphology and Zr concentration; samples with Zr contents greater than approximately 200 ppm showed fine-grained, polycrystalline dendritic morphologies, while samples with Zr contents less than approximately 100 ppm were comprised of agglomerations or linked chains of rhomboidal single crystals. There were few correlations found between morphology, run conditions, and deposit performance.

1. INTRODUCTION

Electrorefining is the heart of the electrometallurgical treatment process for spent nuclear fuel (SNF) currently being demonstrated at Argonne National Laboratory-West (ANL-West). The electrometallurgical treatment process was developed to treat metallic uranium SNF from the Experimental Breeder Reactor-II (EBR-II).[1,2] In the electrorefining step of the process, chopped spent fuel slugs are placed into a molten LiCl-KCl-UCl_3 electrolyte bath and anodically dissolved while purified U metal is cathodically deposited on a bare steel mandrel.

An initial series of runs for checkout of the Mark-IV pilot-scale electrofiner were made using pure depleted U and an alloy of depleted U and 10 wt.% Zr (U-10Zr) as feed material. Detailed metallurgical examinations were performed on the uranium cathode deposits produced in this series of runs; the results are presented in Ref. 3. Significant differences in deposit morphology were observed between deposits produced from the two different feed materials. Deposits produced from pure U feedstock were comprised of chains of uranium crystals with a characteristic rhomboidal shape, while deposits produced from U-10Zr that contained Zr in excess of 0.5 wt% showed fine-grained, polycrystalline features. Higher collection efficiencies (mass of U collected on the cathode divided by the theoretical maximum based on total electrical charge passed) and total deposit weights were observed for the U-Zr deposits. The performance increase was attributed to the better mechanical properties exhibited by the U-Zr deposit morphology.

Metallurgical examinations of samples from cathode deposits continued during the processing of irradiated fuel. The goal was to evaluate the morphologies of deposits produced from irradiated ERB-II fuel for comparison with the morphologies observed for deposits produced from U and U-Zr feedstock. This report presents the results of the investigation. The electrorefiner configuration and different electrorefining operating modes are presented, followed by a description of the range of deposit morphologies observed and the correlations between morphology, chemistry, and performance for the deposits.

2. EXPERIMENTAL PROCEDURES

A. Electrorefiner Description

The cathode deposits were produced by electrofining in the ANL-W Mark-IV electrorefiner (ER) at an operating temperature of 500°C. The ER vessel has a depth and inner diameter of approximately 1 m. At the bottom of the vessel is a pool of molten Cd. The electrolyte, nominally a LiCl/KCl eutectic salt (41 mol% KCl), lies on top of the Cd pool. Approximately 1.6 mol% UCl_3 is dissolved in the electrolyte. Chemically active fission product and actinide elements (e.g., Cs, Ce, Pu) are present in impurity

levels in the salt; their concentrations in the salt increase over time as fuel is processed. The cathode consists of a rotating 67 mm diameter steel mandrel. The cathode deposit size is limited by steel scrapers that are mounted on the vessel walls adjacent to and below the mandrel. The scrapers limit the size of the deposit to a diameter of 0.25 m and a height of 0.23 m. Pieces of the deposit broken off by the scapers fall into the Cd pool and dissolve.

Samples were examined from a total of 36 cathode deposits that were produced from June 1996 through August 1998. The deposits were produced using spent EBR-II U-10Zr driver fuel as ER feed material. The fuel composition was fairly uniform and had been irradiated to approximately 8 at.% burnup. Chopped fuel segments were loaded into perforated fuel dissolution baskets (FDB). Deposits were produced with a direct current power supply operating under controlled current conditions. The power supply was tripped off when a specified maximum cell voltage was reached. Descriptions of the various ER operating modes used to produce the deposits are given in Section B below. A more detailed description of the ER process is given in Refs. 4 and 5.

B. Electrorefining Modes

1. Direct Transport. Most of the deposits examined were produced with the ER power supply configured so that one or two FDB assemblies were anodes, and one or two steel mandrels were cathodes. This transport mode is referred to as direct transport. There were several variations of direct transport used, including the two described below.

- Single anode/single cathode. In this configuration, one FDB assembly was used as the anode, and one steel mandrel was used as the cathode.
- Dual anode/serial cathodes. In this configuration, two FDB assemblies were connected in parallel to the positive lead of a single power supply, and a single steel mandrel was made the cathode. After this cathode accumulated a certain amount of charge (~3000 A-h), it was removed and replaced with a second mandrel.

2. Deposition from the Cd Pool. Some deposits examined were produced by electrotransporting U metal dissolved in the Cd pool (and the vessel walls) to the steel mandrel. In this electrorefining mode, the positive lead of the power supply was connected to the ER vessel so that the vessel and Cd pool were the anode, while a single steel mandrel was the cathode.

3. Mixed Deposition and Direct Transport. Four of the deposits examined were produced using a combination of deposition and direct transport electrorefining modes. For two deposits, direct transport was followed by deposition from the Cd pool. For two other deposits, a three-stage program of deposition, direct transport, and deposition was used.

B. Examination Procedures

After removal of the cathode mandrel from the ER and prior to harvesting of the deposit, small samples of the deposit were taken using remote manipulators. Samples were broken off from several different locations on the deposit (top, middle, bottom), all located on the periphery. The samples were washed with water to remove any highly radioactive, adherent electrorefiner salt. They were then removed from the hot cells and examined. Examination was performed on both exterior surfaces and polished cross-sections of the deposit samples, using scanning electron microscopy (SEM) and metallography. Energy- and wavelength-dispersive spectroscopy was performed on selected samples.

3. RESULTS

A. Deposit Morphologies

A wide range of morphologies were observed for the deposits produced from irradiated EBR-II fuel. All of the morphologies were essentially dendritic in nature; in no instance did the deposit take the form of a uniform surface coating of U on the steel mandrel. However, the macro- and micromorphologies of the dendrites varied considerably. In some deposits, the dendrites were comprised of shiny chains of U crystals, while in others they were dull in appearance with rounded surfaces. These macromorphologies were previously observed for the pure U and U-Zr deposits, respectively.[3] Figure 1 shows a deposit with a shiny, crystalline macro-morphology, and Fig. 2 shows a deposit with a duller appearance.

The micromorphologies observed for the deposit samples examined in the SEM generally reflected the overall deposit morphology. Due to the imaging conditions available in the SEM, it was possible to categorize the morphologies of the deposit samples into several distinct groups, whereas only two distinctions—crystalline and noncrystalline—were possible for the macromorphologies photographed through the hot cell windows. The micromorphologies were categorized according to their qualitative degree of "crystallinity," i.e., the degree to which faceted crystal forms appeared in the sample. On one extreme were fine-grained, polycrystalline dendrites, and on the other were chains of large, rhomboidal single crystals.

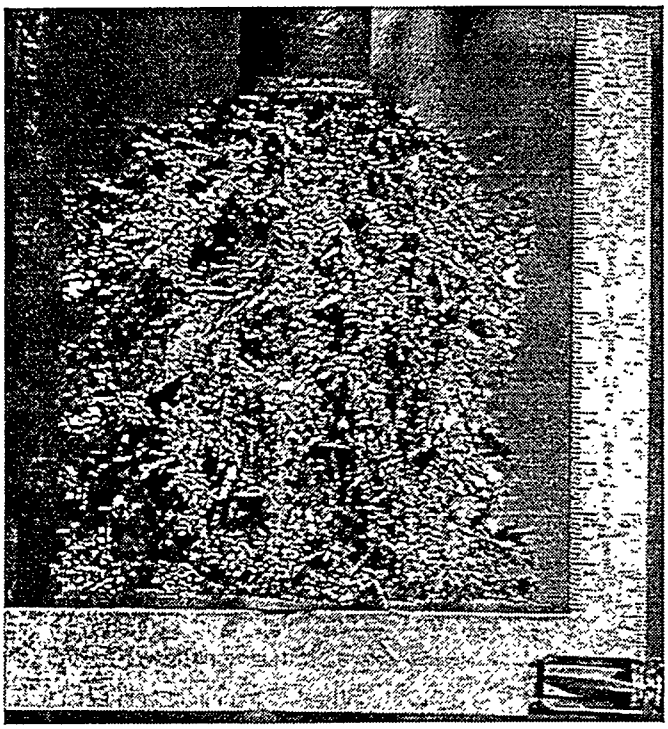

Fig. 1: Example of Deposit with Crystalline Macromorphology (Cathode 73).

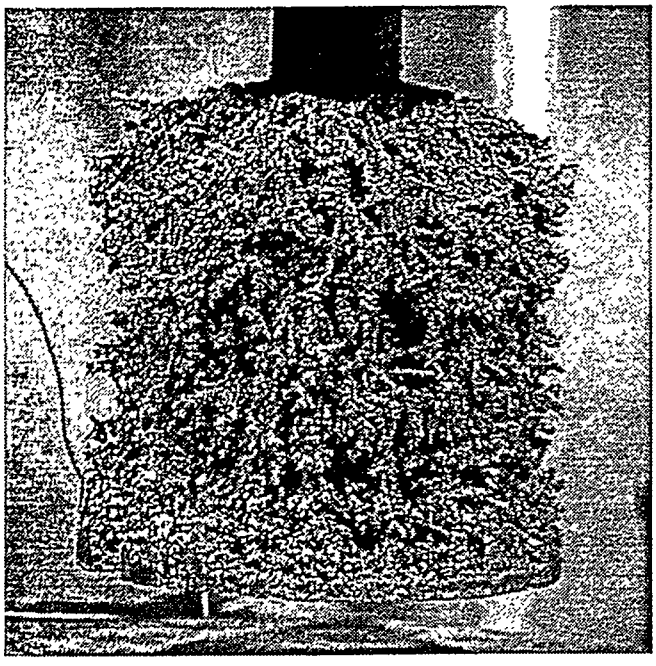

Fig. 2: Example of Deposit with Dull Dendritic Macromorphology (Cathode 88).

The following paragraphs describe and present examples of the micromorphology classifications, in order ranging from least crystalline to most.

1. Polycrystalline Dendrites. The samples showing the least crystallinity were fine-grained, polycrystalline solids. A typical sample with this morphology is shown in Fig. 3. Close views of the dendrite surface showed fine ledges and steps. The polycrystalline nature of this sample was verified by examination of a cross-section. A rounded, convoluted inner structure was observed, typical of polycrystalline samples. The polycrystalline morphology type was observed in the previous investigation[3] for deposits prepared with U-10Zr feedstock.

2. Agglomerations of Nonfaceted Particles. The second morphology class consists of agglomerations of coarse to fine particles, with particle sizes ranging from approximately 25 to 300 μm. For this morphology class, the individual particles are nonfaceted and polycrystalline. An example of this morphology type is shown in Fig. 4.

3. Agglomerations of Blocky Crystals. Agglomerations of blocky, crystalline particles constitute the third morphology class. In contrast to class 2 above, these agglomerations are formed of particles which have smooth surfaces and appear to be single crystals. The crystals in this class are equiaxed, rather than the flat rhombic platelets observed in the classes presented below.

4. Agglomerations of Rhombic Crystals. The only difference between the third and fourth morphology classes is that, in the fourth class, the agglomerations are formed of rhombic-shaped crystals rather than blocky, relatively equiaxed crystals. In many samples both types of crystals were observed. Figure 5 is an example of an agglomeration of rhombic crystals. A cross-section of this sample revealed the complex internal structure commonly observed for the crystals described in Ref. 3.

5. Chains of Rhombic Crystals. Samples in the final morphology class are chains of linked rhombic crystals. This morphology was observed in Ref. 3 for deposits prepared from pure U. The rhombic-shaped crystals observed in this class resemble those shown in Fig. 5, but form extended chains of crystals linked end-to-end.

Each sample was assigned a number (1 through 5) corresponding to its morphology class as defined above. The morphology of some samples did not clearly fit into a single category, but could usually be described as a combination of adjacent categories. These samples were given a rating which was an average of the two different categories. For example, an agglomeration of rhombic and blocky crystals (categories 3 and 4) was given a rating of 3.5.

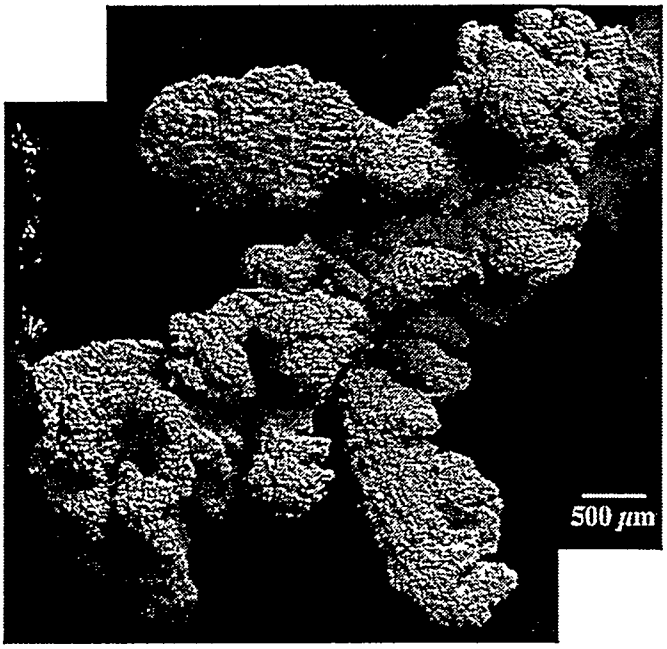

Fig. 3: Example of a Polycrystalline Dendrite (Cathode 88 sample).

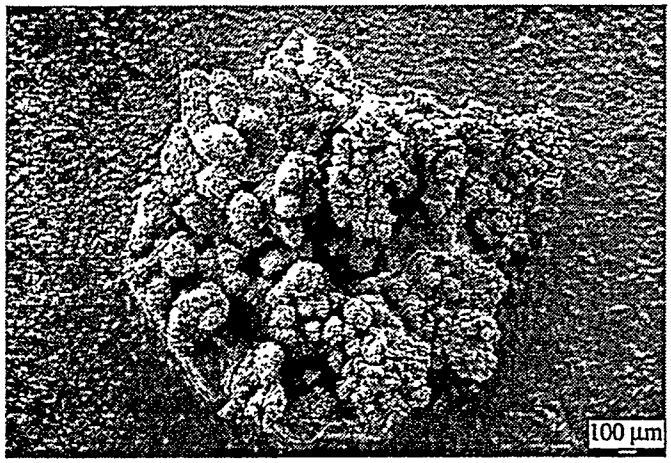

Fig. 4: Example of an agglomeration of nonfaceted particles (Cathode 32 sample).

B. Correlations Between Conditions, Morphology, and Performance

In order to examine the data for possible correlations between run conditions, deposit results, and deposit morphologies, tables listing these parameters for each deposit were generated. A separate table was created for each mode of electrorefiner operation. Tables 1 through 4 show run conditions, results, and morphologies for four different operating modes. Not all operating parameters are

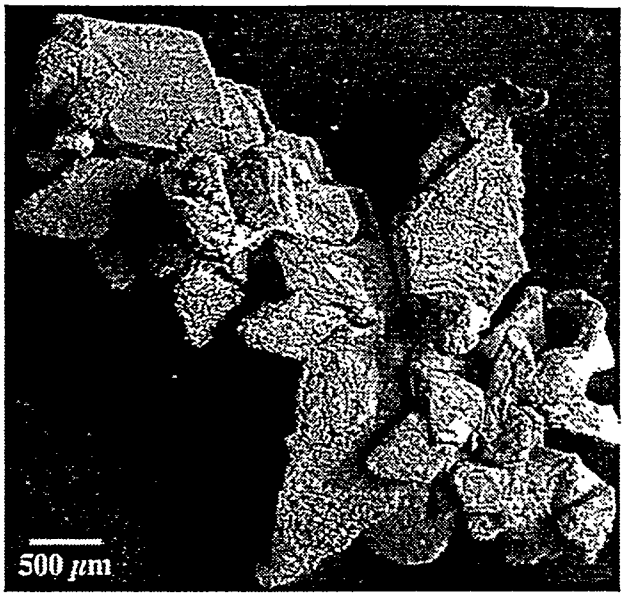

Fig. 5: Example of an agglomeration of rhombic crystals (Cathode 84 sample).

listed, only those which were believed to have the greatest impact on the deposit performance and morphology.

The cathode performance was characterized in terms of the total deposit mass and the U collection efficiency. The runs in each table are sorted in order of decreasing collection efficiency. The macromorphology of the cathodes are listed, along with the average micromorphology category of the one to three deposit samples examined for each deposit (the morphology values correspond to the categories defined above). The average Zr and Cd contents of all the deposit samples are also listed.

Inspection of Table 1 reveals a slight correlation of collection efficiency with morphology for the deposits made using direct transport from a single anode to a single cathode. The correlation between morphology and collection efficiency is not strong, but deposits with collection efficiency greater than 60% tend to be polycrystalline. Their macromorphologies are dull dendritic, and the average morphology category of deposit samples is less than 3. In contrast, the samples from deposits with collection efficiencies less than 60% fall mostly into higher morphology categories representative of crystalline deposits.

Table 2 lists all cathodes made using the dual anode/serial cathode configuration. The first cathodes are identified by the 16.2 kg uranium source; the second cathodes have a 8.1 kg uranium source. Table 2 shows that the first cathodes tended to have a crystalline deposit

Table 1. Run Conditions and Results for Single Anode/Single Cathode Direct Transport

Cathode	66	63	39	49	43	32	48	52	50	61	59	67
U source mass (kg)	8.2	8.2	8.1	8.1	8.1	8.1	8.2	8.1	8.1	8.1	8.2	8.2
Total A-h	2988	3303	3136	4628	3296	3590	4810	3547	2850	3327	3078	3198
Max. cell voltage (V)	0.93	1.18	1.40	0.65	0.84	1.27	0.65	0.65	1.00	0.94	0.54	0.85
Ave. cell voltage (V)	0.65	0.68	1.19	0.42	0.66	1.09	0.42	0.39	0.36	0.80	0.42	0.56
Cathode rotation (rpm)	5	5	20	5	20	20	20	5	20	5	5	5
Anode mix/rotation (rpm)	5	5	75	5	25	75	25	5	25	7	5	5
Cd pool mix (rpm)	20	25	20	25	25	25	25	25	25	25	25	20
Total mass (kg)	8.9	9.07	7.3	10	8	7.9	9.7	6.1	5.5	6.01	3.8	2.9
Recovery efficiency (%)	83	79	67	66	64	61	59	58	52	52	35	26
Macromorphology	Dull dendritic	Dull dendritic	Dull dendritic	Dull dendritic	Dull dendritic	Dull dendritic	Dull dendritic	Dull dendritic	Dull dendritic	Crystalline	Crystalline	Crystalline
Ave. micromorphology	1	1.5	1.3	2.7	1	1.8	3	3	1.8	4	4.3	3.3
Ave. Zr content (wt%)	0.23	0.29	0.28	0.01	0.32	0.90	0.88	0.03	0.11	0.04	0.01	0.01
Ave. Cd content (wt%)	0.65	1.67	2.06	0.69	0.06	1.56	5.78	0.06	0.05	4.93	0.52	0.03

Table 2. Run Conditions and Results for Dual Anode/Serial Cathode Direct Transport

Cathode	77	85	84	74	81	72	71	75	78	82
U source mass (kg)	16.2	8.1	16.2	16.2	16.2	8.1	16.2	8.1	8.1	8.1
Total A-h	3201	2733	3407	3277	3488	2855	3251	3191	3146	2808
Max. cell voltage (V)	0.79	0.99	0.78	0.77	0.78	0.86	1.07	0.84	0.63	0.87
Ave. cell voltage (V)	0.60	0.56	0.63	0.59	0.62	0.54	0.82	0.5	0.39	0.36
Cathode rotation (rpm)	5	5	5	5	5	5	5	5	5	5
Anode mix/rotation (rpm)	5	5	5	5	5	5	5	5	5	5
Cd pool mix (rpm)	20	20	20	20	20	20	20	20	20	20
Total mass (kg)	8.6	7.0	8.5	7.8	8.5	5.6	5.8	4.6	4.1	1.9
Recovery efficiency (%)	72	69	67	66	66	54	49	40	27	18
Macromorphology	Crystalline	Dull dendritic	Crystalline	Crystalline	Crystalline	Dull dendritic	No photo	Dendritic	Dull dendritic	Dull dendritic
Average micromorphology	4	1.5	5	4	5	5	1	1.3	1	1.5
Ave. Zr content (wt%)	0.01	0.08	0.02	0.01	0.01	0.001	0.19	0.16	0.12	0.14
Ave. Cd content (wt%)	0.02	0.01	0.12	0.01	0.02	0.14	0.02	0.02	0.01	0.09

Table 3. Run Conditions and Results for Deposition from the Cd Pool

Cathode	86	46	76	73	36	79	60	83
U source mass (kg)	7	6	12	12	10.9	14	8.8	14
Total A-h	1321	2322	3204	3010	6337	3012	5799	3199
Max. cell voltage (V)	0.56	0.49	0.58	0.58	0.8	0.57	0.69	0.53
Ave. cell voltage (V)	0.4	0.38	0.43	0.4	0.62	0.26	0.37	0.21
Cathode rotation (rpm)	5	20	5	5	20	5	5	5
Anode mix/rotation (rpm)	20	25	20	20	25	20	25	20
Cd pool mix (rpm)	20	25	20	20	25	20	0	20
Total mass (kg)	4.2	6.19	7.7	6	9.7	5	5.1	2
Recovery efficiency (%)	86	77	71	55	52	46	25	18
Macromorphology	No photo	Dull dendritic	Crystalline	Crystalline	Dull dendritic	Crystalline	Crystalline	Crystalline
Ave. micromorphology	4	2.5	4	1	3.5	5	4	5
Ave. Zr content (wt%)	0.03	0.02	0.06	0.04	N/A	0.005	0.003	0.004
Ave. Cd content (wt%)	0.015	0.13	0.96	0.46	N/A	0.025	0.21	0.17

a: Dep. = deposition.

Table 4. Run Conditions and Results for Mixed Deposition and Direct Transport

Cathode	88	37	56	55	82
U source mass (kg)	8/?	8.1/2.4	8.2/8	8.2/8	8.1
Transport mode	DT[1]/Dep.[2]	DT/Dep.	Dep./DT/Dep.	Dep./DT/Dep.	DT
Total A-h	3717	3229/1076	668/2915/1099	643/2956/1085	2808
Max. cell voltage (V)	0.73	1.28/0.78	0.44/0.48/0.26	0.43/0.54/0.26	0.87
Ave. cell voltage (V)	0.45	1.16/0.49	0.37/0.35/0.22	0.38/0.37/0.20	0.36
Cathode rotation (rpm)	5	20	5/5/20	5/5/20	5
Anode mix/ rotation (rpm)	20/5	25	5/5/05	5/5/05	5
Cd pool mix (rpm)	20	25	20	20	20
Total mass (kg)	7.0	6.5	5.2	3.3	1.9
Recovery efficiency (%)	54	43	33	21	18
Macromorphology	Dull dendritic	Dull dendritic	Crystalline	Crystalline	Dull dendritic
Ave. micromorphology	1.3	2.5	3.2	3	1.5
Ave. Zr content (wt%)	0.09	0.71	0.06	0.01	0.14
Ave. Cd content (wt%)	0.04	0.06	4.64	0.21	0.09

1: DT = direct transport.
2: Dep. = deposition.

morphology (category 4 or 5) and higher collection efficiencies than the second cathodes. With one exception, the second cathodes had lower collection efficiencies. The macromorphologies of the second cathodes were all dull and dendritic rather than crystalline, and the micromorphologies tended to be polycrystalline (category 1 or 2). There also appears to be a correlation between collection efficiency and cell voltage (both average and maximum) for the second cathodes, with increasing cell voltage resulting in increasing collection efficiency. The cell voltages of the first cathodes were not varied, so no correlations could be inferred. It was also observed that the cathodes with the three lowest collection efficiencies also have the three highest Zr concentrations in the deposit samples, in sharp contrast to the observation made above for the single anode/single cathode configuration.

Cathodes produced by deposition from the Cd pool are listed in Table 3. For the limited number of cathodes available, there appear to be no correlations between deposition parameters, collection efficiency, and deposit morphology. The final category of cathodes are those which were deposited under a combined program of direct transport and deposition from the Cd pool. Only five cathodes fall into this category. A range of morphologies are observed, but there is no apparent correlation between the run parameters, performance, or morphologies (Table 5).

C. Correlation Between Morphology and Chemistry

The correlation between deposit morphology and chemical composition was examined by plotting the numerical value of the morphology category versus the Zr and Cd contents of the deposit samples. Figure 6 is a plot of morphology category versus Zr content for all deposit samples examined. Although there is considerable scatter, a rough correlation exists between Zr concentration and morphology. Samples with lower Zr contents tend to have more crystalline morphologies (higher morphology category), while the samples with higher Zr contents tend to have less crystalline morphologies (lower morphology category). Samples with rhombic crystal morphologies (category 5) had Zr concentrations less than approximately 100 ppm, and samples with fine-grained polycrystalline morphologies (category 1) had Zr contents greater than approximately 200 ppm. In contrast, there was no correlation between morphology and Cd content.

4. DISCUSSION

A. Deposit Morphologies

The morphologies observed for solid cathode deposits prepared from irradiated fuel fall within the range of morphologies previously observed for pure U and U-Zr deposits.[3] In fact, the previously observed morphologies nicely bracket those presented here. At one extreme are the long chains of rhombic crystals observed for pure U deposits; at the other extreme are the fine-grained, polycrystalline dendrites which were observed for deposits prepared from U-10Zr feedstock. For the irradiated deposits, however, the relatively strict correlation between Zr content and morphology was not observed. The general trends and morphologies at the extremes of Zr content did reflect the earlier observations, in that deposit samples with very little Zr showed morphologies reflective of the pure U deposits and samples with higher Zr showed morphologies reflective of the U-10Zr deposits. In between the two extremes only a weak correlation between Zr content and morphology was observed.

The correlation between Zr content and morphology observed in the present study generally supports the hypothesis presented in Ref. 3 that Zr promotes a polycrystalline deposit morphology by acting as an inhibitor for U electrodeposition. The range of morphologies observed suggests that this effect is complex, with other factors also acting to determine the deposit morphology.

The location of Zr in the samples of deposits made from irradiated fuel generally agrees with the observations of deposits made from nonirradiated U-10Zr feedstock. Zr was commonly found in EDS analyses of the exterior surfaces of deposit samples containing Zr in excess of approximately 200 ppm, and was observed only at the edges of metallographic sections (corresponding to the deposit surface). However, no pure Zr phases were observed in this study, contrary to the previous observations of relatively thick (up to 20 μm) layers of Zr metal dendrites on the deposit surfaces for U-Zr deposits. The lack of Zr phases may be due to the lower overall concentrations of Zr or the more oxidized nature of the samples from the irradiated fuel deposits.

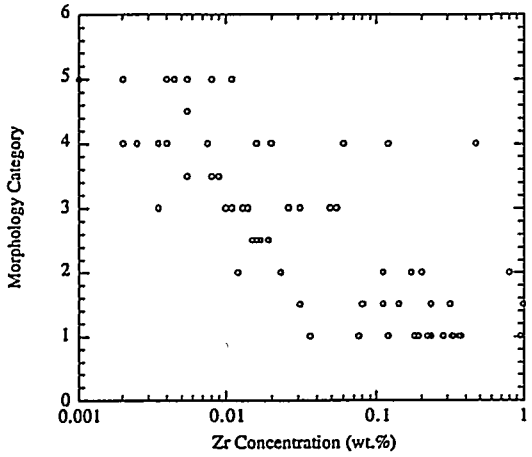

Fig. 6: Plot of morphology category versus Zr content for all deposit samples examined.

B. Run Conditions, Morphology, and Performance

There were very few correlations found between run conditions, deposit morphologies, and deposit performance. The correlations that were observed were weak and contradictory. The best correlation was observed for deposits formed by direct transport from a single anode to a single cathode. For this deposit type, increasing Zr concentration in the deposit and a more polycrystalline deposit morphology correlated with increased collection efficiency. There was no apparent relationship between the run conditions (particularly cell voltage and rotation speeds) and the morphology and Zr content.

For the second electrorefining mode, those deposits produced by direct transport from dual anodes to single, serial cathodes, an apparently contradictory correlation was observed. For the dual anode/serial cathode mode, crystalline deposits with very low Zr contents generally had better performance characteristics than dendritic deposits with higher Zr contents. An additional variable was present in this configuration, in that the first deposit was produced with 16.2 kg of anode feed, while the second deposit was producted with only 8.1 kg of anode feed. The different electrical fields and anodic and cathodic overpotentials present likely account for the different correlation observed.

No correlations were found for the deposits produced by deposition from the Cd pool or by mixed direct transport and deposition. In comparison to deposits produced by direct transport, the range of variables present for these deposits was greater, and the total number of deposits was less.

5. CONCLUSIONS

The morphologies of 65 samples from 36 deposits examined in this study were varied, but fell into a range bounded by the morphologies previously observed for deposits prepared from pure U and U-10Zr feedstock. The morphologies roughly correlated with the Zr concentration in the deposit sample; samples with Zr contents greater than approximately 200 ppm showed fine-grained, polycrystalline dendritic morphologies, while samples with Zr contents less than approximately 100 ppm were comprised of agglomerations or linked chains of rhomboidal single crystals. Zr was found to be present only on the deposit surfaces.

There were few correlations found between morphology, run conditions, and deposit performance. For direct transport from a single anode to a single cathode, there was a weak correlation between improved collection efficiency and a polycrystalline morphology with higher Zr content, but for direct transport from dual anodes to serial cathodes, the opposite appeared to be true. No correlations were observed for deposits produced by deposition from the Cd pool or by mixed direct transport and deposition.

ACKNOWLEDGMENTS

The authors wish to acknowledge the assistance of R.D. Mariani, S.X. Li, and D.E. Vaden in obtaining electrorefiner and deposit information, and E.L. Wood for assistance in preparing the deposit samples. This work was sponsored by the U.S. Department of Energy, Office of Nuclear Energy, Science and Technology, under contract W-31-109-Eng-38.

REFERENCES

1. J.J. Laidler, J.E. Battles, J.P. Ackerman, and E.L. Carls, *Prog. Nucl. Energy*, **31**, 131 (1997).

2. R.W. Benedict and H.F. MacFarlane, *Proc. Third Topical Meeting on DOE Spent Nuclear Fuel and Fissile Materials Management,* Am. Nucl. Soc., Charleston, SC, 651 (Sept. 8-11, 1998).

3. T.C. Totemeier and R.D. Mariani, *J. Nucl. Mater.*, **250**, 131 (1997).

4. S.X. Li, R.D. Mariani, T.J. Battisti, and R.S. Herbst, *Proc. Third Topical Meeting on DOE Spent Nuclear Fuel and Fissile Materials Management,* Am. Nucl. Soc., Charleston, SC 655 (Sept. 8-11, 1998).